FIRE AND MATERIALS '98

5th International Conference

February 1998
San Antonio Tx, USA

Lau, P. W. C.; Zeeland, I. V.; and White, R. 1998. Modelling the char behaviour of structural timber. p. 123–135. In: Proceedings of the Fire and Materials '98 Conference. 23–24 February
In: Proceedings of the Fire and Materials '98 Conference. 23–24 February

interscience communications

MODELLING THE CHAR BEHAVIOUR OF STRUCTURAL TIMBER

Peter W. C. Lau & I Van Zeelaand, Forintek Canada Corp., Canada
& Robert White, Forest Products Laboratory, USA

ABSTRACT

Charring rates for heavy timber based on experimental data have been generally established. The established rates may not be appropriately used for the prediction of failure times of lumber members which are relatively small in comparison to heavy-timber sizes. It is questionable whether a constant rate can be safely assumed for lumber members since the rate is likely to increase once the centre-point temperature of the members starts to rise. This paper presents an empirically-based model of charring rates for Spruce-Pine-Fir (SPF) Machine-Stress-Rated (MSR) *2×4* lumber subjected to a constant—temperature exposure of 500°C, on the basis of test results on 55 specimens. In order that the model can be used with reliability analysis, one of the two model parameters was treated as a *Lognormal* random variable to explain variations observed in the charring rates. Furthermore, the model has been extended to permit evaluations for other lumber sizes and under exposures such as ASTM E119 fire conditions. The model was compared with existing models and used to predict char data found in the literature.

INTRODUCTION

The effect of charring of wood on fire safety of wood-based consturction has been a suject of intensive research for many years. Generally, charring behaviour of wood can either be characterized by the rate of weight-loss (g/s) or by the rate of advance of the char front along a certain axis or dimension (mm/s). The latter definition has been more widely used, particularly in structural fire safety design and analysis, because it lends itself readily to the calculation of cross-sectional "residual area". Typically, the char front is determined on the basis of a series of temperature measurements using thermocouples embedded to different depths of a wood specimen. The position of the char front is then estimated assuming the interface temperature is approximately 300°C.

Charring rates for heavy timber based on experimental data have been generally established. For example, a charring rate of 0.6 mm/min has been determined for glue-laminated timber of medium-density-softwood subjected to ASTME 119[1] standard fire exposures. The charring rates established under ASTM E 119, CAN/ULC S101[2], ISO 834[3], JIS 1301[4] or DIN 4102[5] exposures are quite similar as all these standards have similar temperature-time curves for their fire exposures. For fire safety design of heavy timber structures, Lie[6] recommended use of a charring rate of 0.8 mm/min for light, dry wood, 0.6 mm/min for medium-density softwood, and 0.4 mm/min for heavy, moist wood. In Canada analytical expressions for the fire performance of glue-laminated beams and columns are described in Appendix D-2.11 of the National Building Code of Canada (NBCC). These expressions imply a charring rate of 0.6 mm/min. Swedish Building Code SBN 1976 specifies its charring rate as a function of the *opening factor* of the fire load and recommends a lower-bound limit of 0.6 mm/min and an upper-bound limit of 1.0 mm/min.

It has been questioned whether charring rates established for heavy timber are appropriate for lumber members[7,8]. When wood of "sufficient" mass and volume is exposed to a standad fire-exposure, the rate of charring at the beginning of the exposure is usually more "rapid" than the rate noted for the test. This is because the rate more or less stabilises to a constant rate after the formation of the first few millimetres of char[9,10,11]. Blackshear and Murty[12] attributed the phenomenon to the formation of a steady state of combustion under constant boundary conditions. While the exclusion of the initial non-linear rate data is a

reasonable approach for heavy timber, it maybe too liberal for lumber members because the first few millimeters of char represents a significant proportion of the total cross-sectional area. It is questionable whether a constant charring rate can be safely assumed, given that the rate is likely to increase once the centre-point temperature of the members starts to rise.

Kõnig[8] pointed out that the charring rates assumed by various building codes vary considerably, with values up to as high as 1.0 mm/min. In some codes, higher rates are used to compensate for the loss in strength and modulus of elasticity of the unburnt portion, or to compensate for the loss of section due to the "round-off" effect at corners. The round-off effect refers to the phenomenon that when a wood member is exposed to fire all around, the corners tend to char more rapidly because the heat is coming from both sides of the corner. In other words, the charring rates are calibrated to the loss of load carrying capacity. For lumber members, using a calibrated charring rate to account for both the loss of material due to charring and loss of strength in the unburnt section may prove to be too unreliable. Moreover, the reduction in strength and stiffness of the unburnt portion is not necessarily the same for all grades of lumber because of their wide-ranging strength properties. Under these considerations, the charring rates of such members should be accurately characterized and modelled. The distributional characteristics of charring rate will also be requried if reliability analyses are to be carried out on safety of these members in fires.

This paper presents an empirically-based model of charring rates for Spruce-Pine-Fir (SPF) Machine-Stress-Rated (MSR) *2×4* lumber subjected to a constant—temperature exposure of 500°C, on the basis of test results on 55 specimens. One of the two parameters of the model was considered as a *Lognormal* random variable to explain variations in the Charring rates.

LITERATURE REVIEW

The rate of charring of wood depends on the kinetics of wood combustion, in addition to the exernal fire exposure characteristics. Wood combustion is an extremely complicated process involving the evolution of flammable gases and the diffusion of these gase to and away from the burning surface (mass transfer). Furthermore, heat generated from the burning gases and oxidizing char in turn fuels the decomposition process through conduction of heat inward (heat transfer). These two transfer processes, however, are continuously modified by the effects of the combustion. The decomposition products are functions of temperature, wood species and density, while the transfer processes depend on wood species, moisture content, permeablilty, and other morphological factors. Furthermore, the thermal properties influencing these processes are constantly varying, as is the temperature itself.

Early experimental work by Lawson *et al* [10], Vorreiter[13], followed by Shaffer[14], and then White[15,16], led to several similar empirical models for describing the charring of wood. These models have the general form of either

$$\frac{\partial x}{\partial t} = \eta_1 t^n \qquad [1]$$

or

$$x = \eta_2 t^n \qquad [2]$$

where x is the location of the char-front in the direction of charring $\partial x/\partial t$ is the instantaneous rate of advance of the char front, t is the time, and η_1 and η_2 are regression constants. The exponent n determins whether the rate of charring is increasing ($n>0$), constant ($n=0$), or decreasing ($n<0$) ast time increases. Truax[11] and Vorreiter[13] showed that, with Eqn [2], n attained a value of 1, provided the initial non-linear rate data were excluded from the regression. Schaffer[14] and White[15] expressed their data as a time-location model. It has the form of

$$t = \eta_3 x^n \qquad [3]$$

Models incorporating additional wood parameters such as permeability, density and moisture content have also been derived from the two basic models. A comparison of these models is given in Table 1.

Limited char data are available on some sawn material. One is that of Norén[17], who reported cross-sectional residual areas and t_f distribution of 45-mm-thick by 120-mm-wide spruce lumber exposed to IS0 834 fire exposure. The lumber had a mean moisture content of approximately 18.6% and an average relative density of 0.47. Another is Schaffer's ASTM E 119 char data[18] on *2×4* Douglas-fir lumber.

Discussions concanhg the models, and Norén's and Schaffer's data are given in the latter part of this paper.

Table 1: Empirical charring models for some common softwood wood species

Lawson et al.[10] Spruce timber beams 38 to 50 mm thick exposed to ASTM E 119; moisture content 12%.	$\frac{\partial x}{\partial t} = 1.041\, t^{-0.2}$ where x = location of char front, mm; t = time, min.
Vorreiter[13] Dried spruce plates 10 mm thick placed horizontally and exposed to a flame from underneath.	$x = 0.345 \frac{t^{1.3}}{\rho - \rho_c}$ where x = location of char front, mm; t = time, min; ρ = relative density of wood; ρ_c = relative density of char.
Schaffer I (ASTM E 119 fire exposure)[14] Douglas-fir laminated to 75 mm thick planks and exposed to ASTM E 119; moisture content ranged from 6 to 18%. Similar equations are available for southern pine and white oak.	$t = [(2.27 + 0.046\omega)\rho + 0.33]x$ where x = location of char front, mm; t = time, min; ρ = relative density of wood; ω = moisture content of wood, %.
Schaffer II (constant-temperature exposure)[14] Douglas-fir laminated to 3 inches thick planks and exposed to constant furnace temperatures of 538, 816, 927°C from one side; moisture content ranged from 6 to 18%. Similar equations are available for southern pine and white oak.	$t = -k \ln\left\{1 - \frac{x}{3.0}\right\} \exp\left\{\frac{JE}{RT}\right\}$ where k = $(28.576 + 0.576\ \omega)\ \rho + 4.548$; T = temperature, K; J = 4.184 joules/cal; R = 8.14 joules/(gram-mole•K); E = 3108 cal/gram-mole; x = location of char front, inch; t = time, min; ρ = relative density of wood; ω = moisture content of wood, %.
White[15,16] 63 mm thick specimens from eight species exposed to ASTM E 119; moisture content ranged from 6 to 16%.	$t = k\, x^{1.23}$ where $\ln(k) = -1.7418 + .8485\ f_c + .9388\ \rho + .02\ \omega$ f_c = char contraction factor, dimensionless ρ = relative density of wood; ω = moisture content of wood, %; x = location of char front, mm

EXPERIMENTAL WORK

The experimental work was carried out at the USDA Forest Products Laboratory in Madison, WI. sixty specimens of *2×4* SPF MSR lumber of 4880-mm (16-foot) length were individually placed in a furnace and exposed to a "constant" furnace temperature of 500°C and a constant tensile load of 15570 N (3500 lb) until the specimen failed. The interior dimensions of the furnace were 991 mm wide, 1829 mm long, and 1219 mm high (39 in × 72 in 48 in). It was lined with mineral fibre blankets and heated by eight diffuse-flame natural gas burners that maintained the furnace to within ±10% of any desire temperature.

The furnace had a 229 mm × 508 mm (9 in × 20 in) opening at one end for positioning specimens, one observation window and a removable lid Orientation of the specimens was such that the wider sides were vertical. The length of specimen exposed to the high temperature was 1.8 m. The temperature of exposure was selected to be 500° so that both charring and strength degradation in the inner portion of the specicmen would play an "equal" role in affecting the time to failure of the specimens. The tensile load applied was approximately one third of the fifth percentile of the tension capacity of the specimen testing, the initial weight and moisture content of each specimen was determined. Druing testing, the time until failure of the specimen was recorded. Immediately after failure, the specimen were removed from the furnace and cooled down with water spray. A 25-mm-thick cross-section was taken from each specimen approximately 600 mm from the centre of the specimen. The samples were subsequently used for the determination of the residul area at the time of failure of the specimen using image analysis. The inital relative density of the specimens had a mean value of 0.51 at test and a coefficient of variation of 7.6%. The average fractional moisture content of the oven-dry weight was 0.093 with a coefficient of variation of 3.1%.

Image analysis

Each of the retained sections of the exposed specimens was cleaned with a metal scrapper to remove char particles. Then an image of the cross sectional area of the sample was captured using a microprocessor-based imaging system. Examples of such images are shown in **Figure 1.** The area was computed using software provided with the imaging system. This value is an estimate of the residual area (*A*) with a duration of exposure *t* approximately equal to the time to failure of the specimen. Five specimen were exeluded from this analysis because of missing data. A total of fifty-five values of *A* were obtained.

The images shwon in Figure 1 are typical of residul areas of specimens at various times to failure. As expected, the residual area retained, approximately, a rectangular shape throughout the exposure period but the corners became progressively more rounded. With the execption of the charring at the corners, the depth of char appears to be more or less uniform between the narrow and the wide faces. Charring can, however, be retarded by the presence of a knot because density of knot-wood is generally higher than that of normal wood (see image 863 in Figure 1). Little quantitative work has been done on the effect of knots on charring rate. It should be noted that these charring irregularities will preclude any sensible measurment of the rate of charring in such regions. An "apparent" rate will need to be developed to incorporate the effects due to knots. It is suspected that in wood containing edge knots, the loss of load-carrying capacity due to charring may be insignificant compared to the loss due to elevated temperatures near charring, particularly when it is under tension because of the development of shrinkage cracks. In members subjected to eccentric loading in compression the charring behaviour near knots maybe conveniently neglected because the probability that a "worst" knot defect also occurs in the same location as the maximum stress is relatively low.

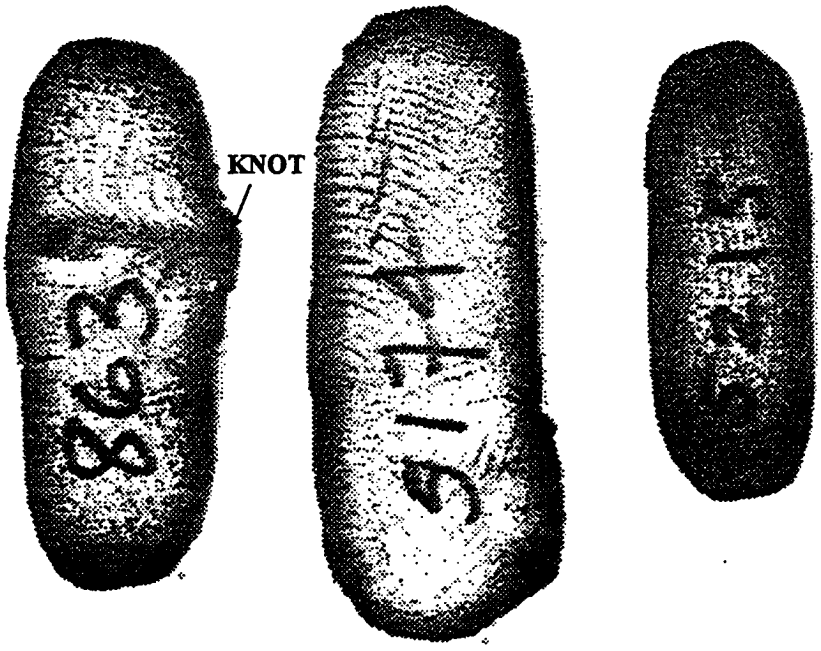

Figure 1: Typical images of residual areas as captured using a computer-based imaging system

MODELLING APPROACH

The residual area *A* is plotted against *t* in **Figure 2,** which indicates that a linear-regression model can be reasonably fitted to these data. The data subject to the linear regression were the residual areas as determined, from which we obtain:

$$A(t) = -1.564\ t + 3022.3 \qquad [4]$$

The average rate of change of the residual cross-sectional area has been estimated from the slope of the fitted regression line, which in turn provides the basis for the derivation of the dimensional rate of charring along the major or minor axis. The regression is shown in **Figure 2** as a light line along with the data. Using this relationship, the "average" rate of change of the residual area is predicted to be -1.564 mm^2/s. In addition, the initial area is predicted to be 3022.3 mm^2, as given by the intercept of the equation. Because this value does not differ "significantly" from the original area of 3080 mm^2 (35 mm by 88 mm) the regression model was modified by forcing the line through the point of 3080 mm^2 at time 0, yielding

$$A(t) = -1.628t + 3080 \qquad [5]$$

This second line is shown in **Figure 2** as a darker line. The slope of the line is -l.628 mm^2/s which represents the rate of reduction of the cross-sectional area from the initial area of 3080 mm^2. This slope is the area charring rate (a).

Norén's char data shown in **Figure 7,** also appear to be linearly related to time of exposure. However, if the trend line through his data is extended back to time zero, the line would have to curve down order to intercept the initial area at time zero. This behaviour was caused by the ISO 834 fire exposure (which is quite similar to ASTM E 119) which initially starts off at toom temperature and reaches only 539°C at 5 minutes. Our exposure was a constant temperature of 500°C.

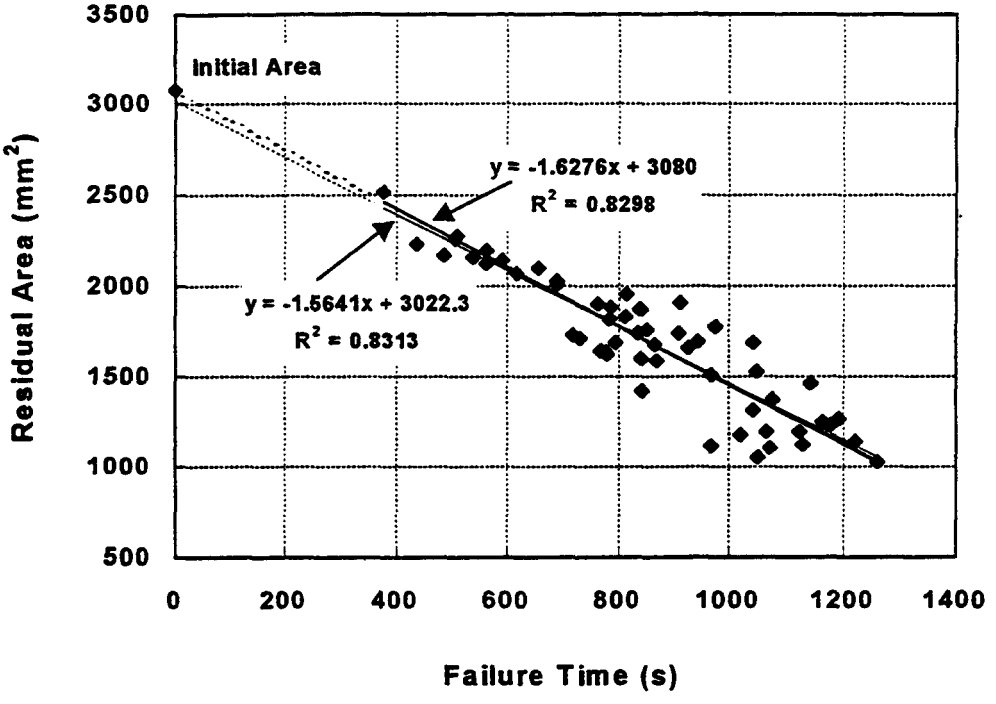

Figure 2: Residual areas versus time of exposure

Dimensional charring Rate

The dimensional charringing by assuming the thicknesses of char in the direction along the major and the minor cross-sectional dimensions are the same. At any time *t*, the residual cross-sectional area ***A(t)*** is given by

$$A(t) = a(t) \cdot b(t) \qquad [6]$$

where *a(t)* and *b(t)* are the residual cross-sectional dimensions at time *t*. Furthermore,

$$a(t) = a_0 - 2\,\delta(t) \qquad [7]$$

and

$$b(t) = b_0 - 2\,\delta(t) \qquad [8]$$

where a_0 and b_0 are the initial uncharred cross-sectional dimensions and $\delta(t)$ is the total depth of char measured from one side as a function of *t*. Taking the derivatives of Eqns [6], [7] and [8], we obtain, respectively

$$\frac{\partial A(t)}{\partial t} = \frac{\partial b(t)}{\partial t} a(t) + \frac{\partial a(t)}{\partial t} b(t) \qquad [9]$$

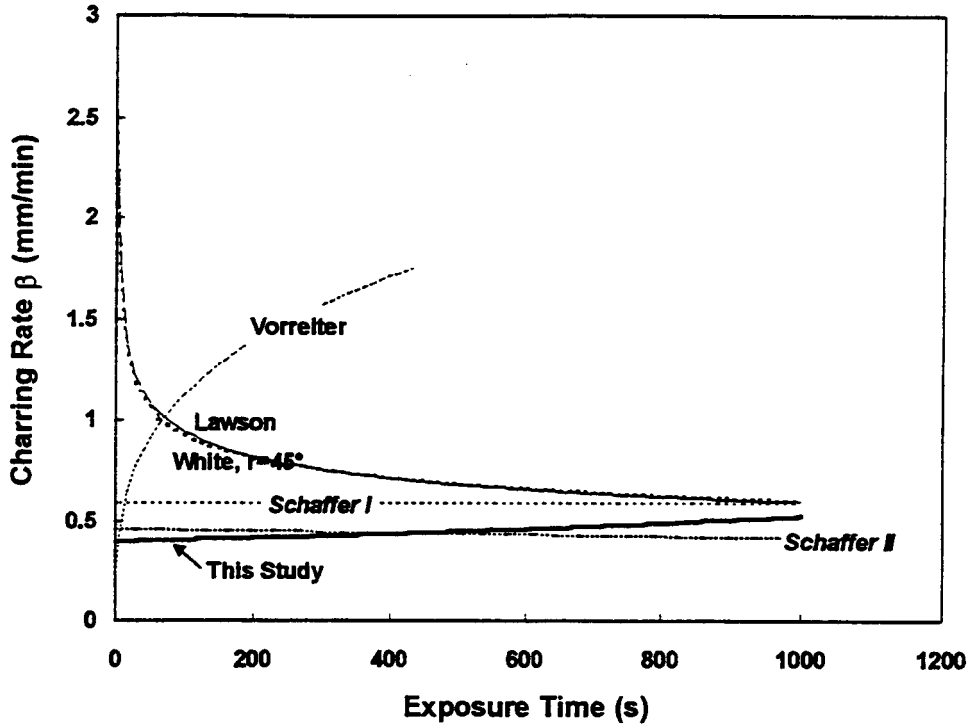

Figure 3: Dimensional charring rates (β) of wood exposed to elevated temperatures

$$\frac{\partial\, a(t)}{\partial t} = -2\frac{\partial\, \delta(t)}{\partial\, t} \qquad [10]$$

$$\frac{\partial\, b(t)}{\partial t} = -2\frac{\partial\, \delta(t)}{\partial\, t} \qquad [11]$$

Substituting Eqns [10] and [11] into [9], and letting $\partial A(t)/\partial t = \alpha$, yields:

$$\frac{\partial\, \delta(t)}{\partial t} = \beta(t) = \frac{\alpha}{-2a_0 - 2b_0 + 8\delta(t)} \qquad [12]$$

where $\partial\delta(t)/\partial t = \beta(t)$ is the instantaneous dimensional charring rate in the transverse direction at time . Solving this first-order differential equation, we obtain

$$\frac{\partial\, \delta(t)}{\partial t} = \beta(t) = -\frac{\alpha}{8}\left[\frac{\alpha\, t}{4} + \frac{1}{16}(a_0 + b_0)^2\right]^{-\frac{1}{2}} \qquad [13]$$

$$\delta(t) = \frac{1}{4}(a_0 + b_0) - \left[\frac{\alpha\, t}{4} + \frac{1}{16}(a_0 + b_0)^2\right]^{\frac{1}{2}} \qquad [14]$$

Eqn[13] and Eqn [14] give the dimensional cahrring rate and char depth expressed as a funtion of *t*, the initial cross-sectional dimensions a_0 and b_0 and *a*. The dimensional charring rate is shown in **Figure 3** with

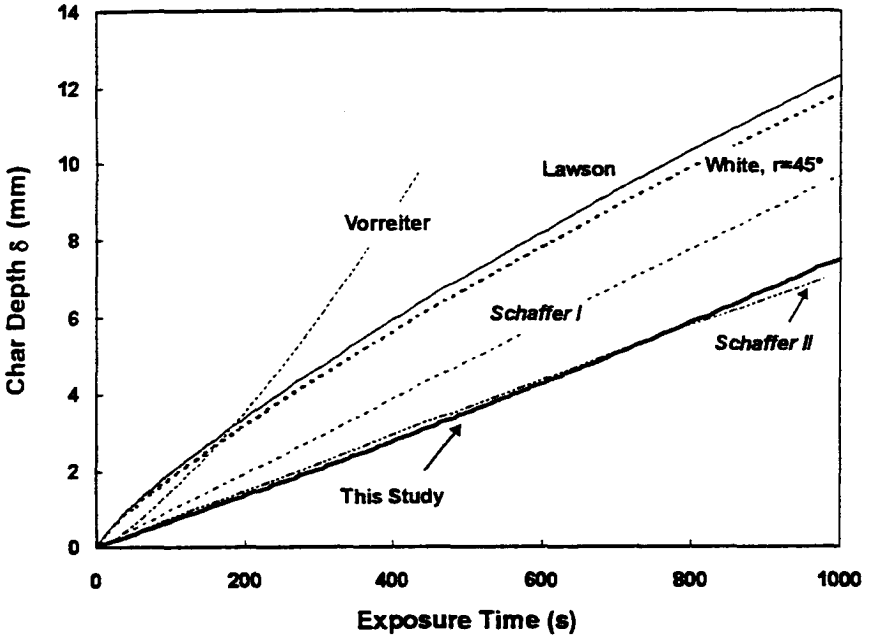

Figure 4: Depth of char (δ) of wood exposed to elevated temperatures

a_0 = *35 mm* b_0= 88 mm and a = -1.628 mm^2/s. From **Figure 3, the** charring rate is predicted to increase gradually overtime, from 0.397 mm/min at $t=0$ to 0.524 mm/min at t =1000s. The average charring rate over that period is calculated to be 0.451 mm/min Compared to the rate of 0.6 mm/min for heavytimber exposed to ASTM E 199 exposure, this value is reasonably lower because the exposure temperature used in this study was only 500°C. The ASTM time curve has the following temperatures: 539°C at 5 min; 704° at 10 min; 843° at 30 min and 927°at 60 min.

Figure 3 also shows the prediction curves of Lawson Vorreiter, Shaffer, and White, whose models are described in Table 1. The char depth (δ) calculated as a function of time on the basis of these models are compared in **Figure 4.** In general, the rates predicted by these models depend significantly on exposure conditions. Some of the observed differences are species, moisture content and size effects; some are attributable to limitations associated with the models. Models developed by Lawson or Vorreiter were not intended to be used to predict the rate of charring at the initial stage of exposure. Those predictions, and therefore their differences at the initial stage of exposure (see Figure 3), are the result of the model choices used rather than of the aetual phenomena.

It is noted that our results and *Schaffer II* (with T = 500+273 K) on both β and δ are similar. *Schaffer II* was developed for constant-temperature exposure based on 75-mm-thick Douglas-fir planks exposed to one side. While the two models predict almost the same char depth up to 1000s (see Figure 4), our model predicts that the dimensional charring rate β is to increase gradually over time whereas *Schaffer II* predicts that it is to decrease gradually. This difference can be attributable to the fact that Shaffer's exposure was from one side only. Both studies suggest that the use of a single charring rate for design purposes may not be appropriate.

VARIABILITY OF CHARRING RATES

In designs based on probabilistic theory where the objective is to limit the probability of failure with respect to the performance function, variability of the design parameters is an important design input. The rate of charring is an important design pammeter but is also high in variability as can be observed in the rate of charring among the 55 specimens exposed (see Figure 2). In these tests, all we know is that the

charring history of an individual specimen bad to pass through two known points – one at the beginning of the exposure and the other at the end of the exposure. Assuming that individual behaviour is also a linear function of *t*, the slope of the line joining the two known points is the bes estimate of this rate. The variability can then be evaluated by examining the distributional charateristics of these slopes.

The results of this examination are plotted in **Figure 5** as a cumulative frequency distribution. The *Normal, Weibull* and *Lognormal* distribution models were fitted to the frequeney distribution data The *Lognormal* model provides the best "fit" to the data. According to Bury[19], *Lognonnal* is an appropriate model for a measurable characteristic whose underlying causes are numerous, independent of each other, and whose "sum" effeet is "multiplicative". The charring variable indeed possesses these characteristics since variability in charring occur naturally as a result of many factors, including mostly, differences immaterial properties – between specimens and within a specimen — such as density, moisture content, permeability, and lignin content[15]. Among these factors, moisture content and density are most important. Variability can also be caused by external factors such as variability of furnace temperaturue. These factors are largely independent of each other. Furthermore, there is evidence found in the models of White[15] and Schaffer[14] to suggest that the combined effect of these factors is multiplicative. For instance, White's charring model implies a multiplicative effect due to char contraction factor *(f_c)*, density (ρ) and moisture content (ω). His charring model relates time *t* to the location of char front *x* by

$$t = mx^b \qquad [15]$$

Where *m* is given by

$$\ln(m) = -1.7418 + 0.8485 f_c + 0.9388\rho + 0.0197\omega \qquad [16]$$

Differentiating *x* of Eqn [15] with respect to *t*, we obtain

$$\frac{\partial x}{\partial t} = \beta = m^{-\frac{1}{b}} b^{-1} t^{\frac{1}{b}-1} \qquad [17]$$

where

$$m = e^{-1.7418} e^{0.8485 f_c} e^{0.9388\rho} e^{0.0197\omega} \qquad [18]$$

It is obvious from Eqn [17] and Eqn [18] that the sum effect of f_c, ρ and ω on β is multiplicative.

***Lognormal* Distribution**

The distribution of charring rate on the basis of residual area $\alpha = \partial A/\partial t)$ is given by the *Lognormal* distribution

$$F_{LN}(\alpha;\mu,\sigma) = \frac{1}{\sigma\sqrt{2\pi}} \int_0^{\alpha} \frac{1}{\alpha} \exp\left\{-\frac{1}{2}\left(\frac{\ln\alpha - \mu}{\sigma}\right)^2\right\} d\alpha \qquad [19]$$

where F_{LN} is the cumulative frequency, σ = 0.106, and μ = 0.486. This function can be used to generate the random value of the area charring rate for reliability analysis.

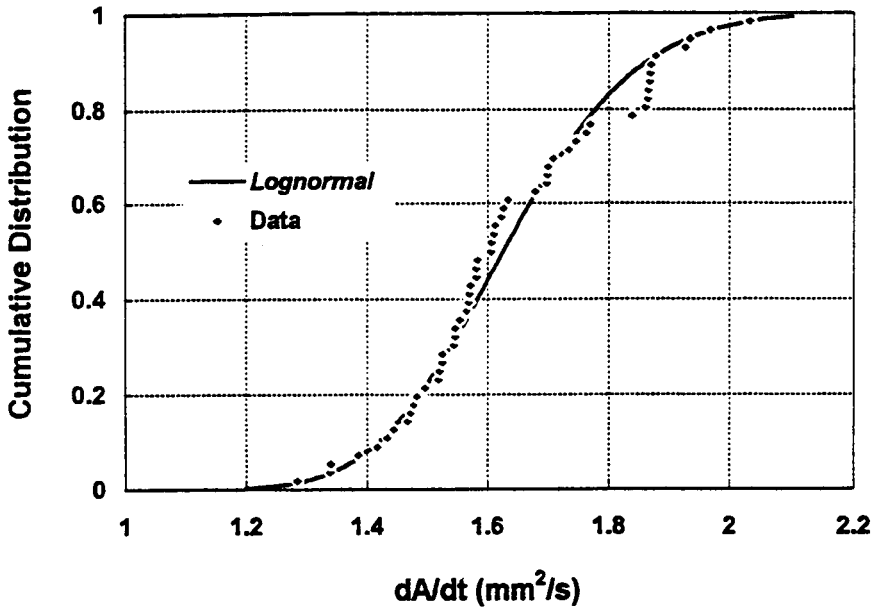

Figure 5: Cumulative frequency distribution of residual charring rates

VARIABLE-TEMPERATURE EXPOSURES

In order that the area-charring model can be used for design purposes or for reliability analysis, it should be extended to predict charring behaviour under other constant temperatures or variable temperatures. Obtaining data for these extensions experimentally would be costly. Instead, we used *Schaffer II* (Table 1) to calibrate a function F— such that $\alpha=\partial A/\partial t=F(T)$ – for use with our model. It was reasoned that the approach is acceptable since the two models are almost identical in their predictions of the average β and δ over a period of 1000s at T =500°C. This approach would incorporate T into the area-charring model as au idepdent variable.

The produre is as follows: for $T > T_c$ = 288°C, we let

$$\alpha(T) = F(T) = a(T - T_C)^b \qquad [20]$$

The values of the coefficients *a* and *b are* then detemined by minimizing the sum of square of differences between predictions of *Schaffer II* (Table 1) on char depth and ours (Eqn [14]), at exposure tepmperatures of 500°C, 600°, 700°, etc., up to 1000°C, and for a period of 1000 s. For $T < T_c$ = 288°C, no charring is assumed to ocour.

Once *a* and *b* are determined, Eqn [20] can be intergated to predict the residual area of lumber exposed either to constant-temperatures or to variable-temperature histories such as ASTM E 119. Note that the coefficents *a* and *b* depend on size because Eqn [14], and on moisture content and relative density of wood because of *Schaffer II.* Figure 6 shows area charring rates predicted as a function of T (constant-temperature) for a *35×88* mm^2 lumber member with a moister content ω =9% and relative density ρ =0.51. Coefficients *a* and *b* for lumber sizes of *2×4, 2×6,* and *2×8,* moisture contents of 8 and 12%, and relative density of 0.40, 0.45, and 0.50, have been determined and are tabulated in Table 2.

Table 2: Coefficients *a* and *b*

Density	Moisture	Lumber Cross-Sectional Dimension (mm)					
ρ	Content	*38x89*		*38x140*		*38x191*	
(oven-dry)	ω, %	*a*	*b*	*a*	*b*	*a*	*b*
0.40	8	-0.171	0.448	-0.179	0.509	-0.201	0.539
	12	-0.154	0.460	-0.164	0.517	-0.185	0.545
0.45	8	-0.142	0.469	-0.154	0.523	-0.174	0.551
	12	-0.128	0.480	-0.141	0.532	-0.160	0.557
0.50	8	-0.121	0.486	-0.134	0.536	-0.153	0.561
	12	-0.109	0.497	-0.122	0.544	-0.141	0.567

Model Testing

Eqn [20] was evaluated based on two sets of data found in literature: (1) Norén's ISO 834 data on spruce[17] with an initial moisture content of 18.6% and a relative density of 0.47, and (2) Scaffer's ASTM E 119 data on Douglas-fir with an initial average moisture content of 7.3% and a relative density of 0.48. The coefficients *a* and *b* were determined for each case as described previously for the initial cross-sectional dimensions of a_0=45 mm and b_0=140 mm in the case of Norén, and 46.8 mm and 90.5 mm in the case of Schaffer. We obtained, for $T > T_c$=288°C, a = -0.11145 and b = 0.54 for Norén. The respective values for Schaffer are a = -0.13079 and b = 0.49304.

Then, replacing T with $T(t)$, the ISO 834 temperature-time curve, in Eqn [20], where

$$T(t) = T_0 + 345\log_{10}(8t+1) \qquad [21]$$

and separating the variables by A and t, then performing an integration with respect to the variable on each

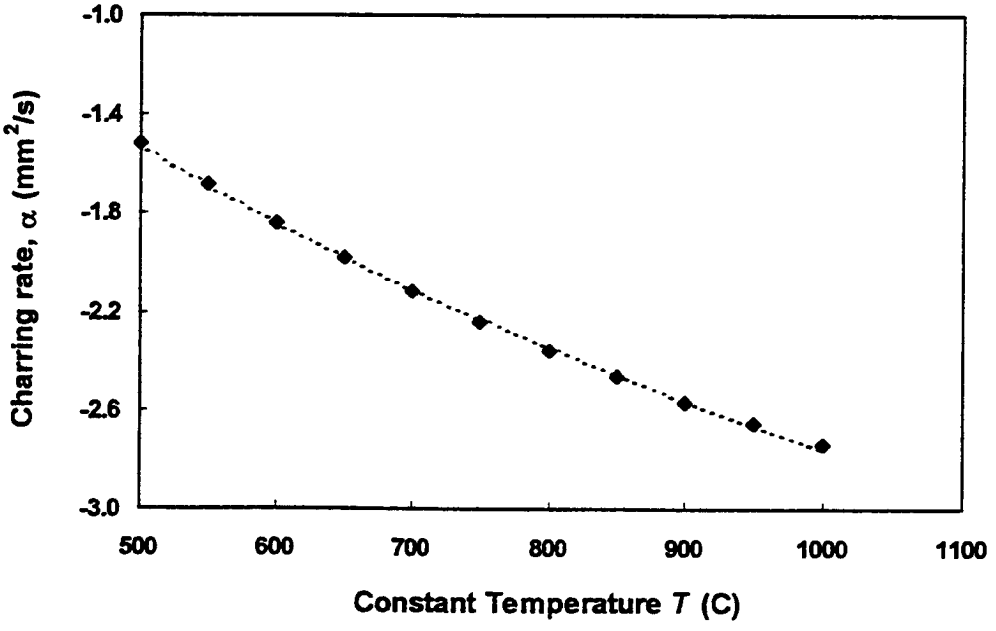

Figure 6: Area charring rate calibrated using Schaffer II (Table 1)

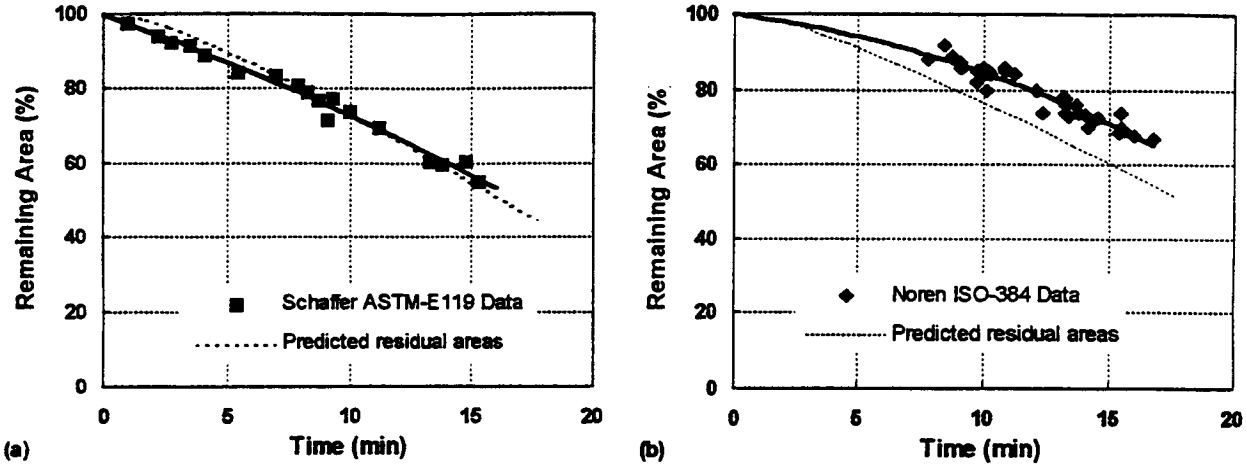

Figure 7: Model predictions of Schaffer's ASTM E 119 Douglas-fir data (a) and Norén's ISO 834 spruce data (b)

side of Eqn [20], we obtain

$$\int_{A_0}^{A_R} dA = \int_{t_0}^{t_R} a\left(345\log_{10}(8t+1)+T_0-T_C\right)^b dt \qquad [22]$$

The residual area A_R at time t_R is given by

$$A_R = A_0 + \int_{t_C}^{t_R} a\left(345\log_{10}(8t+1)+T_0-T_C\right)^b dt \qquad [23]$$

where t_c is the time it takes to reach the temperature of T_c (which can be computed from Eqn [21]). In the case of Schaffer, the temperature curve was assumed to be also given by Eqn [21].

The results of this calculation and the two set of experimental data are shown in **Figure 7.** As shown in **Figure 7a,** Schaffer's *2x4* data are reasonably predicted while those of Norén **(Figure 7b)** are over-predicted. The over-prediction is probably the result of a significant difference in permeability between the spruce Norén used and the Douglas-fir used in Schaffer's experiment in developing his seoond model. Because the moisture content of Norén's data was high — 18.6% — permeability probably played a significantly role in affecting the rate of charring.

CONCLUSIONS AND RECOMMENDATIONS

This paper reports the charring behaviour of 55 specimens of 2×4 SPF lumber exposed to 500°C in a furnace. A linear model of the residual area was developed yielding a constant rate of charring of 1.628 mm^2/s. The corresponding "dimension" charring rate is found to be a function of time with an average value of approximately 0.45 mm/min (0.0075 mm/s). The rate is predicted to increase gradually with time of exposure, to a value of 0.52 mm/min at an exposure time of 16 min. In comparing these dimensional charring rates to rates determined by several other experiments reported in the literature, the results are reasonable. Finally, the variability of the area charring rate among the specimens tested can be characterized by a *Lognormal* distribution. The distribution can be used as an input to reliability analysis of a structural member exposed to a 500°C environment by tinting the residual cross-sectional area as a variable.

An area-chiming model, which incorporates an existing model by Schaffer to express the rate of charring as a function of temperature of exposure, has been developed to predict residual areas of lumber exposed to constant-temperature or variable-temperature histories. The model was found to predict, with reasonable accuracy, a sample of 45×120 mm^2 spruce lumber exposed to ISO 834 fire exposure. This model is capable of predicting char depth as a function of time given a variable-temperature history. It is recommended that this model be improved to account for the permeability effect in wood with high moisture contents.

ACKNOWLEDGEMENT

Forintek Canada Corp. would like to thank its industry members, Natural Resources Canada (Canadian Forest Services), and the Provinces of British Columbia, Alberta, Québec, Nova Scotia and New Bunswick, for their guidance and financial support for this research.

REFERENCES

1 ASTM E 119-95a, Standard Method of Fire Endurance Tests of Building Construction and Materials. American Society for Testing and Materials, Philadelphia, PA (1995).

2 CAN/ULC-S101-M89, Standard Method of Fire Endurance Tests of Building Construction and Materials. Underwriters' Laboratories of Canada, Scarborough, Ontario, Canada (1989)

3 ISO 834, Fire-Resistance Tests—Elements of Building Construction. International Standards Organization, Geneva, Switzerland (1975).

4 JIS 1301, fire resistance tests standard published by the Japan standard organization JIS.

5 DIN 4102, fire resistance tests standard published by the German standard organization DIN.

6 Lie, T.T., A method for assessing the fire resistance of laminated timber beams and columns, *Canadian J. of Civil Eng* 4:161-169 (1977).

7 Hay, R., Fire damage sensitivity criteria for wood fibre structures: Proposal for a new international standard, *Proc., 1990 International Timber Engineering Conference*, ed. by Hideo Sugiyama, Science University of Tokyo, Japan, Vol. 1, pp. 100-109 (1990).

8 Kõnig, J. Modelling the effective cross section of timber frame members exposed to fire, paper presented at 1991 meeting of the International Council for Building Research Studies and Documentation, Working Commission W18A – Timber Structures (1991).

9 M. Jean, The behaviour in fire of wood and wood-based materials. Presented at the IUFRO Fifth Conference on Wood Technology. U.S. Forest Products Laboratory, Madison, WI (1963).

10 D. I. Lawson, C. T. Webster and L. A. Ashton, Fire endurance of timber beams and floors. *J. Structural Eng.* **30**(2), 27-34 (1952).

11 T. R. Truax, Fire research and results at US Forest Products Laboratory. *United States Forest Service Research Report No. 1999*, Madison, WI (1959)

12 P. L. Blackshear, Jr., and K. A. Murty, The measurement of physico-chemically controlled ablation rates. Tech. Rep. No. 1 (AD 285 460). Univ. of Minn. Inst. of Technology, Minneapolis (1962).

13 L. Vorreiter, Combustion and heat insulating losses of wood and fibreboards. *Holzforschung* **10**(3), 73-80 (1956).

14 E. L. Schaffer, Charring rate of selected woods transverse to grain. United States Forest Service Research Paper FPL 69, Forest Products Laboratory, Madison, WI (1967).

15 R. H. White, *Charring Rates of Different Wood Species*, PhD dissertation, University of Wisconsin, Madison, WI (1988).

16 R. H. White, and E. V. Nordheim, Charring rates of wood for ASTM E119 exposure. *Fire Technology*, Febrary 1992.

17 J. B. Norén, Failure of structural lumber when exposed to fire. In *Proc. 1988 International Conference on Timber Engineering, ed.* by R. Y. Itani, pp. 397-406, Washington State University.

18 E. L. Schaffer, The effects of Fire on Selected Structural Timber Joints, Master Thesis, University of Wisconsin, Madison, WI (1961).

19 K. V. Bury, *Statistical Models in Applied Science*, John Wiley & Sons, New York (1975).